Current Concepts on the Diagnostic Use of MIBG in Children

Barry L. Shulkin and Brahm Shapiro
Division of Nuclear Medicine, University of Michigan Medical Center, Ann Arbor; and Department of Nuclear Medicine, Ann Arbor VA Medical Center, Ann Arbor, Michigan

Metaiodobenzylguanidine (MIBG) was developed 18 yr ago for scintigraphic imaging of the adrenomedullary tumors pheochromocytoma and neuroblastoma. Many studies have shown the usefulness of this agent for the management of patients with neuroblastoma or pheochromocytoma, and the ^{131}I-labeled form was recently approved by the Food and Drug Administration for use in the U.S. This article summarizes our current concepts on the diagnostic use of MIBG in children. The radioisotopes available for labeling of MIBG and related compounds, the dosimetry, metabolism and mechanisms of uptake and retention are discussed. Our protocols for imaging both ^{131}I-MIBG and ^{123}I-MIBG, along with the normal distribution of these compounds, are reviewed. The use of MIBG for the management of neuroblastoma, and comparisons with other radiotracers available for imaging neuroblastomas are also addressed.

Key Words: metaiodobenzylguanidine; neuroblastoma; pheochromocytoma; children

J Nucl Med 1998; 39:679–688

It has been 18 yr since the development of metaiodobenzylguanidine (MIBG) by Wieland, 16 yr since the first reports of successful sympatho-medullary tumor localization in humans and 3 yr since the approval of the ^{131}I-labeled form of this agent by the Food and Drug Administration (FDA) for the diagnostic imaging of neuroblastoma and pheochromocytoma (*1–3*).

Neuroblastoma is the third most common malignancy of childhood, exceeded in frequency only by primary brain tumors and leukemia (*4*). These highly malignant tumors arise from primitive neuroectodermal cells. Neuroblastomas comprise about 10% of pediatric tumors and account for about 15% of cancer deaths in children. The annual incidence is nine cases per million white children younger than 15 yr of age and about half that in nonwhite children. These are neoplasms of young children, with 75% occurring by age 4 or younger, and 50% by age 2. They may originate wherever sympathetic nervous tissue is found and tend to present at advanced stages. Approximately 85% are associated with increased excretion of urinary catecholamines or catecholamine metabolites.

Attempts to develop radiotracers that concentrate in adrenomedullary tissues began nearly 30 yr ago. Initial efforts centered on catecholamines and their precursors. Radiolabeled inhibitors of the enzymes of catecholamine synthesis were also studied. A successful approach involved the use of ganglionic blocking agents (*5*). Korn et al. (*6*) investigated radioiodinated bretylium analogs. Paraiodobenzylguanidine localized sufficiently within the canine adrenal medulla to enable imaging. Attempts to image human pheochromocytomas with this agent were unsuccessful, probably because the patients examined did not have pheochromocytoma (*5*). Subsequent work by Wieland was conducted with the meta-isomer, MIBG, which has less deiodination in vivo (*1*). The adrenal medulla of dogs and primates were scintigraphically visualized, followed by the localization of pheochromocytomas in humans (*1,2*). Our earliest studies in neuroblastoma were inconclusive, probably because the first patients studied were heavily pretreated and subsequently either did not have neuroblastoma or the tumors were largely necrotic. The majority of subsequent studies performed elsewhere and at our institution were positive and were confirmed in multiple series conducted worldwide (*7,8*).

Radiolabels

Radioiodinated MIBG is an aralkylguanidine that bears structural similarity to the neurotransmitter and catecholamine hormone norepinephrine and the ganglionic blocking drug guanethidine. Radioiodination with ^{131}I, ^{123}I, ^{125}I or ^{124}I is performed by exchange reaction at 142–145°C (*9*). Free iodine is removed by ion-exchange chromatography. Characteristics of commercially available ^{131}I-MIBG available within the U.S. are: radiochemical purity > 90%, radionuclide purity > 99% at the time of release, specific activity 3.3 mCi/mg and a shelf life of 14 days after manufacture. Iodine-123-MIBG produced at the University of Michigan has radiochemical purity > 90%, radionuclide purity > 98%, specific activity of ~ 57 mCi/mg and a shelf life of 24 hr following synthesis (information provided by Neil A. Petry, RPh).

Iodine-125-MIBG has been used for animal biodistribution and in vitro studies, as well as for intraoperative probe studies and therapy (*10*). Iodine-124-MIBG has been used for PET imaging (*11*). This has the potential for quantification of dosimetry before ^{131}I-MIBG therapy. Fluorine-18 and ^{76}Br analogs have also been synthesized for PET imaging (*12–14*).

Astatine-211, an alpha emitter, has been used to label 3[^{211}At]astato-4-fluorobenzylguanidine, a compound structurally related to MIBG, in order to produce a radiopharmaceutical with desirable characteristics for radionuclide therapy of neuroblastoma (*15*).

Dosimetry

The properties of selected radionuclides that have been used to label MIBG and analogs and their dosimetry are depicted in Tables 1 and 2. Initial scintigraphic experience with MIBG was obtained using the ^{131}I-labeled compound. Iodine-131 has suboptimal physical imaging properties and dosimetry, which greatly limit the activities that can be administered. Despite this, sensitivity and specificity have been quite high (Table 3). The use of ^{123}I for labeling takes advantage of the better physical properties of ^{123}I for imaging, allows higher activities to be administered with favorable radiation dosimetry and greater photon flux resulting in higher count, higher quality planar images and permits the performance of SPECT. There is evidence to suggest that this results in higher sensitivity for

Received Oct. 31, 1997; accepted Nov. 2, 1997.
For correspondence or reprints contact: Barry L. Shulkin, MD, Director, Pediatric Nuclear Medicine, MCHC F 3313 Box 0229, University of Michigan Medical Center, Ann Arbor, MI 48109.

TABLE 1
Properties of Radionuclides That May Be Used to Label MIBG and Its Analogs

Radionuclide	Mode of decay	$T_{1/2}$	Principal photon energy	Principal particulate emissions	Remarks
^{123}I	Gamma, EC	13.2 hr	159 keV	Low-energy Auger electrons	Near ideal gamma camera imaging agent; various accelerator routes of production; supply and cost remain problems. Permits SPECT.
^{125}I	Gamma, EC	60 day	35 keV	Multiple low-energy Auger electrons	Widely used for animal and in vitro studies. May have utility for the therapy of micrometastases and intraoperative tumor location with probe detectors.
^{131}I	Gamma, β^-	8.05 day	364(637)* (723)* keV	Multiple β^- (69–190 keV)	Less than optimal for gamma camera imaging. Suitable for therapy of larger tumor deposits. Convenient compromise agent, approved by FDA.
^{18}F	β^+	110 min	511 keV†	β^+	Label for MFBG and FIBG.
^{11}C	β^+	20 min	511 keV†	β^+	Label for HED and epinephrine.
^{76}Br	β^+	16.2 hr	511 keV†	β^+	Label for MBrBG that has been used for PET of cardiac autonomic innervation.
^{211}At	α	7.2 hr	77–92 keV‡ 500–900 keV§	α	Label for MABG that has potential for α therapy.

*Minor but still significant emission.
†Annihilation photon
‡X-rays from α decay
§Gamma rays from α decay
EC = electron capture; MIBG = meta-iodobenzylguanidine; FIBG = fluoro-iodobenzylguanidine; HED = hydroxyephedrine; MBrBG = meta-bromobenzylguanidine; MABG = meta-astatobenzylguanidine.

detection of disease, although this may be due to higher photon flux from the higher administered activity rather than from ^{123}I per se (*16*). The dosimetry of ^{123}I-MIBG is such that 10 mCi may be administered with the same radiation dose as 0.5 mCi of ^{131}I-MIBG. The useful photons available for imaging at various times after a diagnostic dose of ^{131}I and ^{123}I MIBG are described in Table 4.

Metabolism

After intravenous injection, the majority of activity from injected ^{131}I-MIBG is excreted through the urinary tract: 40%–55% in 24 hr and 70%–90% in 96 hr. Most of this is in the form of intact ^{131}I-MIBG, while small fractions are excreted as ^{131}I-4-hydroxy-3-iodobenzylguanidine (HIBG), ^{131}I-meta-iodohippuric acid and ^{131}I-metaiodobenzoic acid. A small, but chemically uncharacterized portion of the activity, is excreted into the gut, which may give rise to bowel visualization that can be reduced by laxatives and enemas if necessary (*17*). The metabolism of MIBG labeled with other radioiodines and analogs labeled with other radiohalides may be assumed to be similar.

Cellular Mechanisms: Uptake and Storage

MIBG is a tracer of the so-called type 1 amine uptake and granular storage mechanisms. It enters adrenomedullary tissue by two pathways. One is a specific, energy-requiring, sodium-dependent, low-capacity, high-affinity amine uptake mechanism (type 1), and the other is a nonspecific, energy-independent diffusional mechanism (*18*). Once transported into the neuroblastoma cell, the majority of MIBG remains within the cytoplasm free of granular storage (*19,20*). In pheochromocytoma cells, where there is a large population of catecholamine storage granules, MIBG is actively transported into the granules by an active reserpine-sensitive uptake mechanism. MIBG does

TABLE 2
Radiation Dose Estimate Comparisons from Iodine-123- and Iodine-131-MIBG in Patients of Various Ages*

	Estimated radiation dose (Rads/mCi)											
	Newborn		1 yr		5 yr		10 yr		15 yr		Adult	
Organ	^{131}I	^{123}I	^{131}I	^{123}I	^{131}I	^{123}I	^{131}I	^{123}I	^{131}I	^{123}I	^{131}I	^{123}I
Adrenals	14.1	0.55	20.0	0.59	12.9	0.37	9.62	0.266	6.66	0.185	4.8	0.137
Bladder	20.7	0.89	5.5	0.41	4.4	0.33	2.81	0.222	1.85	0.152	2.8	0.237
Liver	5.5	0.48	2.4	0.23	1.3	0.122	0.89	0.085	0.63	0.059	0.44	0.044
Ovaries	32.6	1.44	15.2	0.64	6.7	0.314	3.7	0.189	2.33	0.115	1.18	0.074
Bone marrow	10.4	0.63	4.4	0.29	2.26	0.155	1.44	0.104	0.89	0.067	0.74	0.059
Spleen	26.6	1.55	10.0	0.63	5.5	0.348	3.48	0.229	2.22	0.152	1.55	0.111
Testes	10.7	0.48	4.1	0.20	2.2	0.111	1.33	0.067	0.81	0.044	0.70	0.037
Thyroid†	555.0	29.6	370.0	21.1	203.5	11.1	88.8	5.18	59.2	3.40	34.0	2.072
Whole body	10.7	0.52	4.4	0.22	2.22	0.122	1.37	0.077	0.85	0.048	0.89	0.053

*Estimated radiation doses are based on the distribution data of Swanson et al. (65) and were adapted from Stabin M, *personal communication*, 1981.
†Assumes no iodides have been administered. Iodides will reduce thyroid dosimetry to ~ 1%–2%.

TABLE 3
Comparison of Results of MIBG Scintigraphy for Suspected Neuroblastomas

Study site	Number of cases	True-positive	False-positive	True-negative	False-negative	Sensitivity	Specificity	−PDA	+PDA	Prevalence
Michigan recent summary of data (*67*)	45	32	0	5	8	80	100	39	100	89
Amsterdam, Holland (*68*)	47	39	0	6	2	95	100	75	100	87
Villejuif, France* (*69*)	24	14	0	4	6	70	100	40	100	83
Philadelphia, PA (*70*)	13	8	2	3	6‡	57	60	60	80	74
Copenhagen, Denmark (*71*)	37	20	3	14	0	100	82	100	87	54
Tubingen, West Germany (*72*)	5	4	0	1	0	100	100	100	100	80
Munster, West Germany (*73*)	7	3	0	3	1	75	100	75	100	43
Odense, Denmark (*74*)	9	4	0	5	0	100	100	100	100	43
Hamburg, West Germany (*75*)	19	63	0	–	7	90	–	–	90	100
Heidelburg, West Germany (*76*)	13	10	0	3	0	100	100	100	100	77
Niigara, Japan (*77*)	6	4	0	0	2	67	–	–	100	67
Valencia, Spain (*78*)	36	11	0	25	0	100	100	100	100	31
Durban, South Africa (*79*)	12	6	0	6	0	100	100	100	100	50
Summary of world-wide experience presented at	37	32	1	–	4	100	–	–	97	100 (patients)
international Workshop of Pediatric Oncology (Rome, 1986) (*80*)†,§,¶	121	85	1	–	35	70	–	–	99	100 (sites)

*Majority of studies performed with ^{123}I-MIBG.
†Results listed by sites of disease.
‡In four cases, tumor was present but had matured to ganglioneuroma or ganglioneuroblastoma.
§Majority of studies performed with ^{131}I-MIBG.
¶Includes three gangliomas and three ganglioneuroblastomas (all of which were positive by MIBG).

not bind to postsynaptic adrenergic receptors nor is it degraded by the enzymes, which metabolize catecholamines. The retention of MIBG in neuroblastomas reflects the rapid reuptake of the radiotracer that has escaped the cell. This is quite different from the mechanism of retention of MIBG in pheochromocytoma cells where retention largely reflects intragranular storage of the compound. In neuroblastoma cell cultures, uptake of MIBG can be enhanced by differentiating compounds such as gamma interferon and retinoic acid (*21*).

Because the retention of MIBG in neuroblastomas is highly dependent on an intact, active catecholamine and related compound transport system, drugs that interfere with uptake may impair visualization. A variety of agents have been described that impair visualization of pheochromocytomas (Table 5) (*22*). Many of these are used to treat conditions rarely found in the pediatric population. In clinical practice, the drugs most likely to interfere with visualization of neuroblastomas are over-the-counter cough and cold preparations that contain pseudoephedrine or phenylpropanolamine. Before injection of the MIBG tracer, parents should be specifically asked about recent administration of all prescribed drugs and over-the-counter cough and cold preparations that might not be considered by parents as drug treatments. The effects of many drugs on MIBG uptake by the sympathoadrenal system have not been formally investigated in cell culture, experimental animals or in man.

TABLE 4
Relative Useful Photons from Iodine-131-MIBG and Iodine-123-MIBG Taken up by a Pheochromocytoma

Time after administration (hr)	Relative useful photons* 0.5 mCi (^{131}I-MIBG)	10 mCi (^{123}I-MIBG)
0	1	80.0
24	0.92	22.4
48	0.84	6.4
72	0.77	1.6

*Baseline reference of 0.5 mCi ^{131}I-MIBG at 0 hr = 1. These calculations assume that:
1. Gamma camera efficiency for ^{131}I = 20%.
2. Gamma camera efficiency for ^{123}I = 80%.
3. The number of useful photons escaping from body with ^{123}I is equal to that with ^{131}I, without taking into account somewhat greater attenuation of lower-energy ^{123}I photons.
4. The photon yield of ^{123}I (84%) equals photon yield of ^{131}I (82%).
5. Tracer uptake is instantaneous, and retention is complete, in pheochromocytoma, and that distribution is identical for ^{131}I and ^{123}I-MIBG (*51*).

Image Acquisition

The protocol for MIBG imaging at the University of Michigan has evolved with 15 yr experience using this agent and now includes the following features:

Patient Preparation. Iodides, usually in the form of saturated solution of potassium iodide, are administered to reduce thyroidal accumulation of free radioiodine, preferably beginning the day before injection. Perchlorate has also been used but must be repeated as long as substantial quantities of free radioiodine are present in the circulation. Patients and/or parents are always asked about exposure to potential interfering agents. If none is noted, an indwelling intravenous line is established. The dose of MIBG is administered by slow intravenous injection over 90 sec. Because of the propensity for neuroblastoma to disseminate, images from the head to the distal lower extremities should be obtained.

Iodine-131-MIBG Scintigraphy. Scintigraphy is performed 1, 2 and occasionally 3–4 days after the intravenous administration of 0.5–1.0 mCi/1.7 m^2 body surface area (~7 μCi/kg to 15 μCi/kg). Conjugate views of the head, neck, chest, abdomen and pelvis are acquired for 100,000 counts or 20 min, whichever comes first. Images at later times suffer from lack of recognizable normal anatomy, as structures with physiologic uptake tend to lose activity with time. However, tumors often become more evident over time with the reduction in the surrounding background. Anterior views of the extremities are adequate. Alternatively, a low-speed, whole-body scan could suffice. A large field of view, dual-head gamma camera with

TABLE 5
Drugs Known or Expected to Reduce MIBG Imaging

Known to reduce uptake of MIBG	
Drug	**Mechanism**
Sympathomimetics	Depletion of storage vesicle contents
Phenylephrine	These drugs occur in numerous nonprescription decongestants and diet aids: their use should be excluded
Phenylpropanolamine	
Pseudoephedrine, ephedrine	
Antihypertensive/cardiovascular	
Labetalol	Inhibition of catecholamine uptake Depletion of storage vesicle contents
Reserpine	Depletion of storage vesicle contents Inhibition of vesicle active transport
Calcium-channel blockers	Uncertain (also enhance retention of previously stored norepinephrine and MIBG by blocking Ca^{++}-mediated release from vesicles)
Tricyclic antidepressants	Inhibition of catecholamine uptake
Cocaine	Inhibition of catecholamine uptake

Expected to reduce uptake of MIBG	
Drug	**Mechanism**
Sympathomimetics	Depletion of storage vesicle contents
Amphetamine and related compounds	
Beta-sympathomimetics*	
Dobutamine	
Dopamine	
Metaraminol	
Atypical antidepressants	Inhibition of catecholamine uptake
Maprotiline	
Trazodone	
Antipsychotics (major tranquilizers)	
Phenothiazines†	Inhibition of catecholamine uptake
Thiozanthines	
Butyrophenones	
Antihypertensive/cardiovascular	
Adrenergic neuron blockers	Depletion of storage vesicle contents Competition for transport into vesicles

*Systemic use. Effect unlikely with aerosol administration.
†Occasionally used as antiemetic/antipruritic agents.

high-energy collimators is preferred. In addition to analog images, digital data should be stored and available to allow computer enhancement and adjustment of background. Simultaneous dual-isotope acquisition or subtraction studies after imaging after administration of other agents (e.g., ^{99m}Tc-MDP) is possible because of the difference in energy windows between ^{131}I and ^{99m}Tc.

Iodine-123-MIBG Scintigraphy. Scintigraphy is performed to obtain both planar and tomographic images (*23,24*).

For planar imaging, anterior and posterior spot views from the top of the head to the proximal lower extremities are obtained for 10 min 24 hr and 48 hr following injection of 10 mCi/1.7 m^2 of body surface area (~150 μCi/kg, maximum 10 mCi). Anterior views of the distal lower extremities are sufficient. A large field of view dual-head gamma camera with low-energy collimators is preferred.

For SPECT imaging, most patients receiving ^{123}I-MIBG also undergo SPECT at 24 hr, using a single- or multiheaded camera with a low-energy collimator. The camera is rotated through 360°, 120 projections at 25 sec per stop. Data are reconstructed using filtered backprojection with a Butterworth filter and a cutoff frequency of 0.2–0.5.

Normal Scintigraphic Findings

The normal in vivo distribution of ^{131}I-MIBG includes the salivary glands and nasopharynx, the heart (uptake into which is often quite intense in children), the liver, spleen and bladder (*25*). Faint uptake of free radioiodine may be seen in the thyroid depending on the level of thyroid blockade. The same structures are depicted more clearly with ^{123}I-MIBG and more frequently bowel activity, lungs, normal adrenal medullae and supraclavicular muscle uptake that can be mistaken for disease (*23,26*). Cerebellar visualization has been reported, although we have not observed uptake in this area on diagnostic images (*27*). Other areas of uptake are considered abnormal until proven otherwise (*28*).

Use of MIBG Scintigraphy

MIBG has been shown valuable in the management of patients with neuroblastoma from the initial diagnostic evaluation all the way through monitoring patients who have completed therapy.

Diagnosis. The MIBG scan may occasionally be useful in establishing the diagnosis of neuroblastoma where the lesion is inaccessible for easy biopsy or the patient is too ill. Uptake of MIBG by a mass in the appropriate clinical circumstances for all practical purposes indicates the lesion is of neuroendocrine origin and may help distinguish neuroblastoma from the other small blue round cell tumors of childhood (Figs. 1, 2). Having a preoperative diagnosis before surgery may help in the planning of the nature and extent of the operation.

Neuroblastoma may be associated in 20%–50% of children with the rare opsoclonus-myoclonus syndrome (also called the dancing eyes of Kinsbourne's syndrome). Because the tumor may be occult and because the prognosis of the paraneoplastic and the postviral or idiopathic varieties differ, MIBG scintigraphy may be useful to screen the entire patient for neuroblastoma deposits (*29,30*).

Prognosis. The initial MIBG scan may be useful in predicting the response to therapy. Suc et al. (*31*) found that the risk of failing to achieve a complete remission after four courses of chemotherapy was sevenfold greater in patients with more than four deposits of MIBG avid neuroblastoma at diagnosis in children greater than 1-yr-old.

Staging. The accurate depiction of the full extent of disease spread and distribution are essential before therapy for both prognostic classification and therapeutic decisions (Figs. 3,4). Prognosis is highly dependent on the stage of the disease. The intensity and extent of therapy depends on the staging. Focal lesions may require localized therapy even in extensive (Stage 4) disease. MIBG scintigraphy may reveal disease foci that are otherwise not detected and thus upstage the disease. We found this happens most frequently in the thoracolumbar spine, where bone scans may appear misleadingly unremarkable. In many instances, the MIBG scan reveals all the tumor deposits delineated by full combinations of other techniques and also reveals other lesions not demonstrated by any other modality (*32*). Heterogeneity of uptake may occur in a minority of cases and thus complicate interpretation although this is uncommon.

Response to Therapy. Most neuroblastomas show good initial responses to therapy, although complete remissions are challenging to sustain. It is, thus, essential to serially evaluate the extent of disease during therapy, at the completion of each protocol and during prolonged follow-up (Fig. 5). The ability to screen the entire patient in a single noninvasive procedure is clearly advantageous. The uptake of MIBG, which depends on

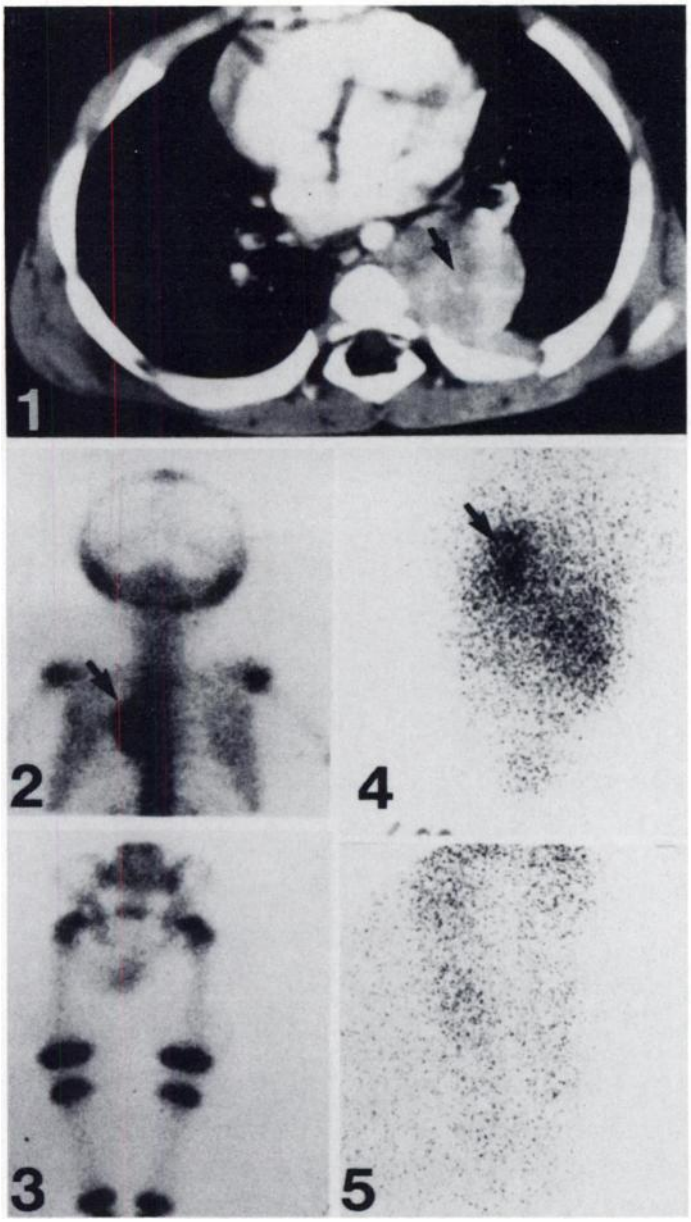

FIGURE 1. A 1-yr-old boy with 2-mo history of cough (panel 1). CT scan of the chest shows a left posterior thoracic tumor (arrow) with scattered calcification (panels 2, 3). Bone scan: posterior views of the head and chest, and pelvis and legs show uptake of ^{99m}Tc-MDP within the primary tumor (arrow), and no evidence for osseous metastatic disease (panels 4, 5). Iodine-131-MIBG scan at 48 hr. Posterior view of the chest and anterior view of the lower extremities shows uptake within the tumor (arrow). Assymetry in uptake in the lower extremities was positional in nature. Note the difference in uptake in the lower extermities of this patient, representing muscle uptake, from the pattern seen in the patients with diffuse (Figs. 3 and 4) and focal (Fig. 5) tumor involvement of bone.

a sophisticated, relatively specific, functional property of neuroblastoma is strong evidence of viable tumor, although occasionally ganglioneuromas may also show uptake. For the most part, this property helps distinguish post-therapy fibrosis and necrosis from residual viable neoplasm. After bone marrow transplantation, MIBG is useful in monitoring for relapse, although the combination of CT and MIBG provides even greater accuracy (*33*).

We previously described the results of MIBG scintigraphy in 330 cases compiled from 13 publications from 8 countries (*8,34–39*). An updated summary is listed in Table 3. The sensitivity for detection of disease was 87% and specificity 94%. The positive predictive value was 98% and the negative

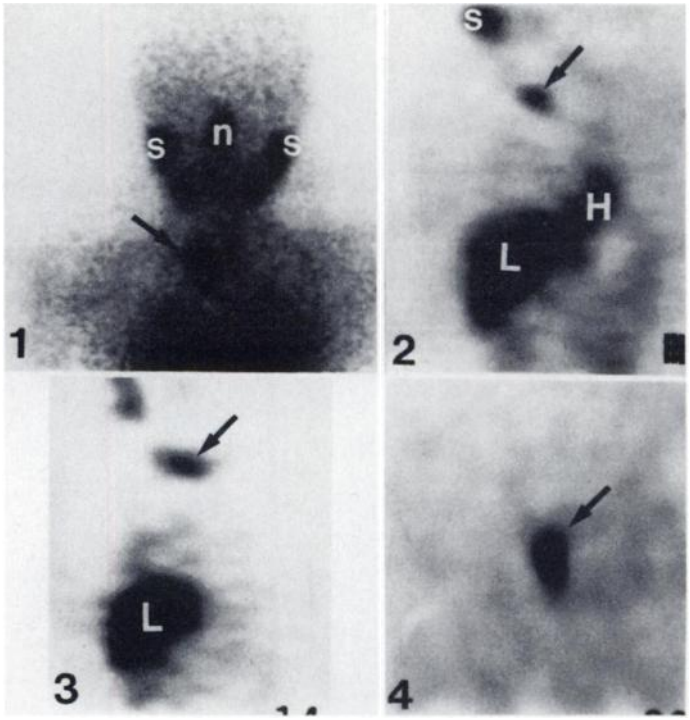

FIGURE 2. An 8-yr-old boy with residual thoracic neuroblastoma after resection. Iodine-123-MIBG scan at 24 hr (panel 1). Anterior planar image shows uptake into the tumor (arrow) and normal uptake in the salivary glands (s) and nasopharynx (n) (panels 2–4). Coronal, sagittal and transverse SPECT sections show uptake in the tumor (arrow) and normal uptake in the liver (L) and heart (H), and provides three-dimensional localization of the lesion.

predictive value 70%. Only one study has found MIBG not to be valuable for the monitoring of neuroblastoma (*40*).

Iodine-131 Versus Iodine-123 MIBG

A minor controversy exists regarding the use of ^{123}I versus ^{131}I MIBG (*9*). In the U.S., only the ^{131}I-labeled form is commercially available. However, many academic institutions produce ^{123}I-MIBG for local use under an Investigational New Drug exemption granted by the FDA. As previously stated, the images obtained from ^{123}I-MIBG studies have higher counts and greater quality, providing more ready recognition of the sites of normal uptake. While limited data exist regarding the efficacy of ^{123}I-MIBG versus ^{131}I-MIBG, one study showed the same number of lesions identified by both techniques, while another study suggests greater numbers of lesions identified with ^{123}I-MIBG scintigraphy (*16,41*). It is unclear, however, if staging was altered by the discovery of greater numbers of lesions. We prefer to use ^{123}I-MIBG for its greater image clarity. However, we do not hesitate to use ^{131}I-MIBG for diagnostic imaging if the ^{123}I-labeled agent is unavailable. Although ^{131}I-MIBG images suffer from the suboptimal characteristics of the ^{131}I radiolabel, ^{131}I-MIBG remains an excellent agent for the scintigraphic depiction of neuroblastoma.

For ^{123}I-MIBG, the roles of SPECT and planar imaging have been reviewed (*24,42*). One study found no increase in the number of lesions detected when SPECT was added to planar imaging, but did find an increase in the certainty that suspected abnormalities on planar imaging were indeed abnormal. We, however, did find an increase in the number of abnormal sites on SPECT imaging and better anatomic localization of the lesions.

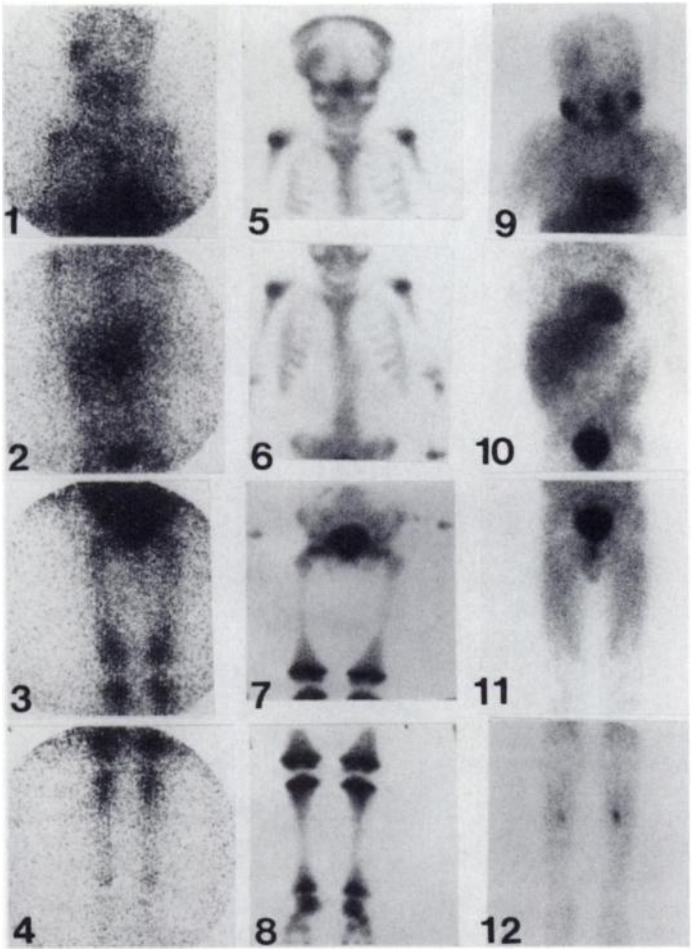

FIGURE 3. A 3-yr-old boy with leg pain (panels 1–4). Iodine-131-MIBG scan at 48 hr. Anterior views show extensive metastases throughout the axial and appendicular skeleton (diffuse pattern). Vertebral lesions were more apparent on posterior images (not shown) (panels 5–8). Bone scan at presentation demonstrates abnormal uptake in the right frontal skull and only subtle symmetric abnormalities about the knees and ankles (panels 9–12). Iodine-123-MIBG scan at 24 hr. Anterior views after extensive chemotherapy show considerable resolution of disease. Residual abnormalities are present in the skull and proximal tibias.

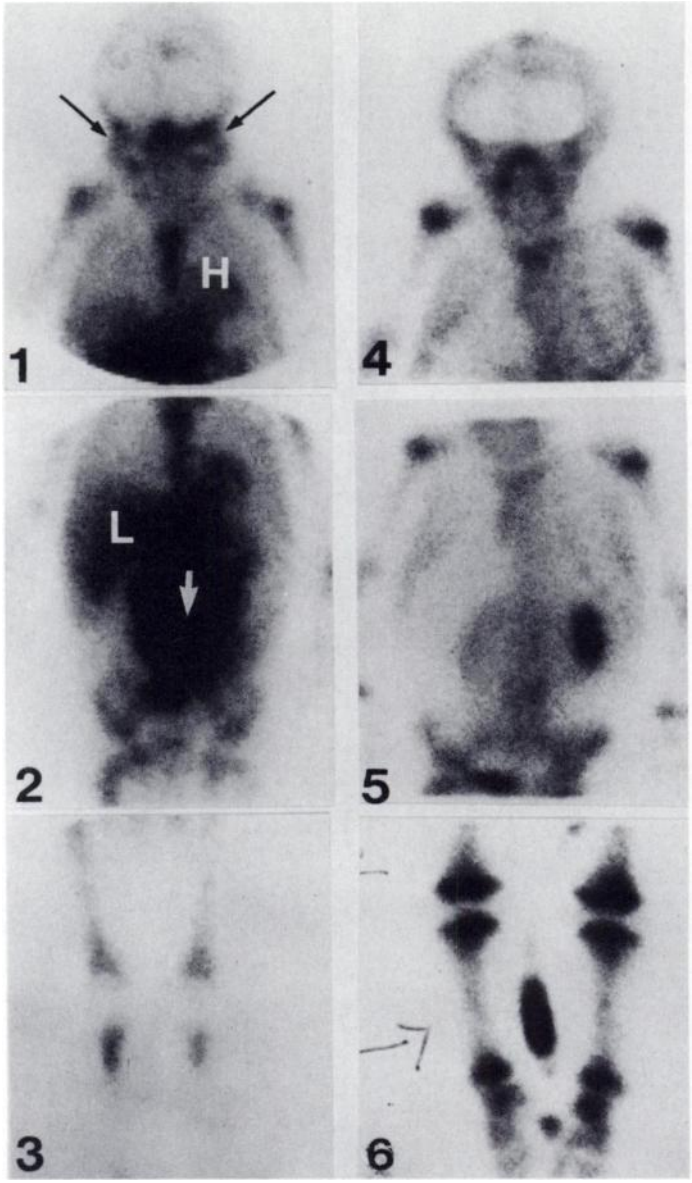

FIGURE 4. A 2-yr-old boy with left leg pain and limping (panels 1–3). Iodine-123-MIBG images at 24 hr. Overlapping anterior views show abnormal uptake in the orbits (black arrows, "raccoon eyes"), normal uptake in the heart (H) and liver (L), a large abdominal tumor with intense uptake (white arrow), and extensive uptake in the femurs and proximal tibia (diffuse pattern) (panels 4–6). Bone scan anterior views. The findings are much less impressive. The symmetry of uptake in the orbits, pelvis, and knees poses a diagnostic challenge. Note the partial obstruction of the left kidney, which is encased by the tumor.

Comparison of MIBG with Bone Scan

The bone scan has traditionally been a technique that permits screening of the entire skeleton for neuroblastoma deposits (*32*). Many primary neuroblastomas accumulate ^{99m}Tc-MDP, and neuroblastoma is a common cause for extraskeletal uptake of bone-seeking tracers in the pediatric population (Fig. 1). We found extraskeletal uptake of MDP in approximately 40% and MIBG uptake in 80% of patients with soft-tissue masses demonstrated on CT examination (*43*).

The depiction of osseous lesions depends on excitation of an increased bone remodeling response within bone. Until the introduction of MIBG, the bone scan provided the most useful determination of the extent of skeletal metastases. As the metastatic lesions of neuroblastoma usually originate with the bone marrow cavity, bone scan changes may underestimate the early stages of metastatic spread (Figs. 3 and 4). Because of the propensity of neuroblastoma to localize in the metaphyseal region adjacent to the epiphyseal plates, sites of normally increased uptake of bone seeking tracers, metastatic involvement may be difficult to appreciate. Additionally, considerable attention to scan technique and positioning is critical to distinguish normal metaphyseal uptake from neuroblastoma involvement, particularly when this is symmetrical. Similarly, the bone scan may remain abnormal due to increased bone turnover and remodeling even after the successful eradication of viable tumor. The bone scan is sensitive to a wide range of other pathological processes including trauma and infection, which may occasionally complicate the interpretation. Gordon et al. (*44*) reported eight false-negative ^{123}I-MIBG scans for skeletal involvement in 44 children although about 60% more lesions were found with MIBG scintigraphy than with bone scanning. Our study of 77 patients, using ^{131}I-MIBG, found complete concordance between MIBG scanning and bone scanning for the presence or absence of skeletal disease (*43*). A nearly twofold greater number of skeletal lesions were evident on MIBG scanning. No patients with normal bone scans had MIBG studies, indicating tumorous bone involvement. Another study of ^{123}I-MIBG and skeletal scintigraphy showed more skeletal lesions with ^{123}I-MIBG and several false-positive foci on bone scintigraphy (*45*).

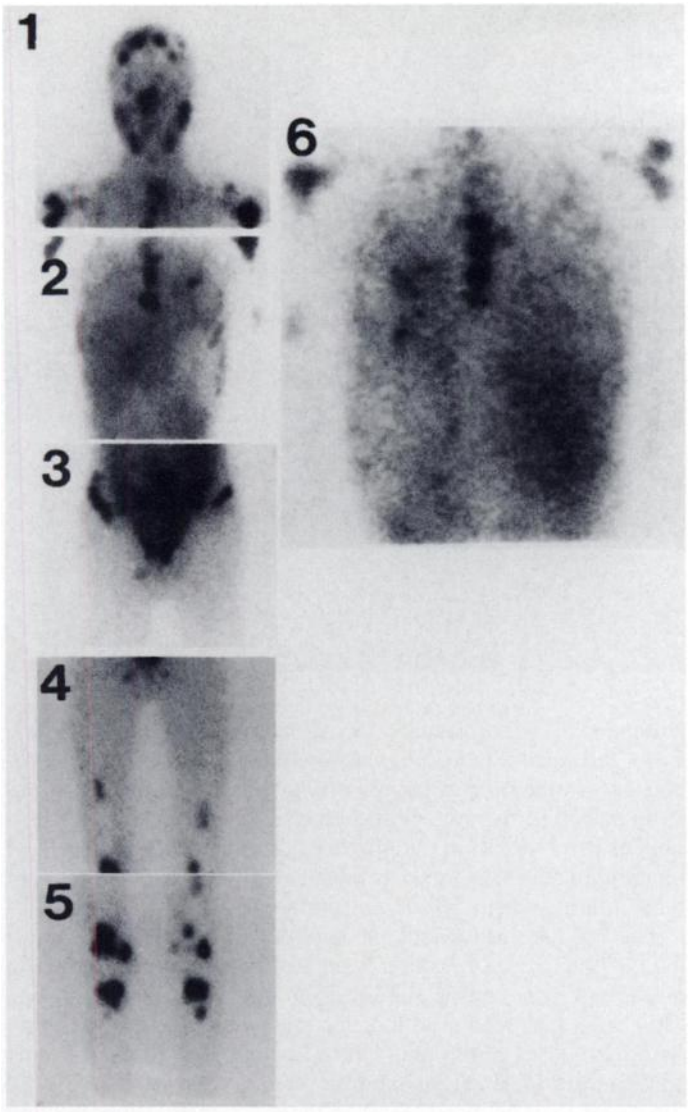

FIGURE 5. A 15-yr-old boy with recurrent neuroblastoma after bone marrow transplantation. Iodine-123-MIBG scan at 24 hr. Overlapping anterior views (panels 1–5) and posterior chest-abdomen (panel 6). There are multiple deposits of tumor within the skull, humeri, upper and mid thoracic spine, ribs, pelvis, femurs and tibiae (focal pattern).

MIBG and bone scanning have been compared to bone marrow aspiration (*46*). When only a single site is sampled, which in this article is the iliac crest, MIBG scintigraphy indicated bone marrow infiltration by neuroblastoma in considerably more patients than did bone marrow aspiration. The aspiration samples from eight patients with diffuse bone uptake of MIBG all contained neuroblastoma. The aspiration samples from 16 patients with both diffuse and focal uptake of MIBG within bone contained histologic evidence of tumor in only eight. There were only two cases of neuroblastoma demonstrated within bone in 91 studies with no MIBG uptake within bone. The authors concluded that bone marrow aspiration biopsy in patients with diffuse skeletal uptake of MIBG does not add additional information since a negative aspiration biopsy fails to rule out bone marrow involvement.

MIBG, MRI and bone marrow biopsy have also been compared (*47*). Bone marrow biopsy is subject to sampling error since only a small portion of the skeleton is sampled. MIBG and MRI may show bone marrow involvement in areas not accessible to bone marrow biopsy, and MRI may show more bone marrow lesions than MIBG. However, the specificity of MRI is not clear nor are the effects of therapy on MRI findings.

Imaging Postradionuclide Therapy. MIBG imaging after therapy with ^{131}I-MIBG is routinely undertaken in institutions where such experimental therapy is performed. The very high photon flux from the residual activity, and the inherent delay from the time of administration of therapy to the time when the remaining activity falls to levels that allow the patient to be released, contribute to the very high quality of images despite the unfavorable imaging characteristics of the ^{131}I radionuclide. When the body burden of ^{131}I-MIBG declines to levels below 30 mCi, whole-body images and spot views are acquired for 5–10 M counts on at least one occasion. Tomography may be performed and may be of quite high quality if the very high counting rate is fully used to collect high information density images. We and others have often observed additional foci of disease on post-therapeutic scans not visible on diagnostic images, consistent with the concept of dose responsive imaging (*48*).

Specificity. In the appropriate clinical context, MIBG is highly specific for neuroblastoma. We have recently described the results of MIBG scintigraphy in a variety of childhood tumors other than neuroblastoma from five referral centers in three countries (*49*). Most children were studied because of initial suspicion that their tumors were indeed neuroblastoma. Overall, 100 children were included. All had negative scans except for 1 of 2 with infantile myofibromatosis, 1 of 2 with neuroendocrine carcinomas, 1 of 2 pancreatoblastomas and 1 of 10 primitive neuroectodermal tumors. The more frequently occurring solid tumors of childhood most likely to be confused with neuroblastoma in the very early stages of diagnosis, such as Wilms tumors and soft-tissue sarcomas, consistently failed to concentrate MIBG (0/14 and 0/15, respectively). Thus, MIBG is only rarely concentrated by non-neural crest tumors. The specificity of MIBG for neuroblastoma in the appropriate clinical context is $> 95\%$.

Childhood pheochromocytomas are very uncommon compared to neuroblastoma, but these tumors usually also accumulate MIBG (Fig. 6) (*50,51*). Childhood pheochromocytomas usually manifest typical findings (hypertension, "spells," palpitations, headaches, pallor, tremor) and occur in children considerably older than most patients with neuroblastoma. Plasma and/or urinary catecholamines and metabolites are usually diagnostic. Nonetheless, it is essential to locate all tumor deposits since complete extirpation is the only means of cure.

Radiotracers Related to MIBG. Several analogs of MIBG have been synthesized for investigation of the sympathetic innervation of the heart and for neuroendocrine tumor imaging and therapy. These include: ^{123}I-amino iodobenzylguanidine (AIBG), ^{18}F-fluorodopamine, ^{18}F-fluronorepinephrine, ^{18}F-fluorometaraminol, ^{11}C-hydroxyephedrine (HED), ^{11}C-epinephrine (EPI), ^{11}C-phenylephrine and fluoro-metaiodobenzylguanidine (FIBG). Only three have been investigated in patients with neuroendocrine tumors. AIBG is concentrated in deposits of pheochromocytoma (*52*). This compound was synthesized to permit easy ^{123}I labeling as a kit form. However, blood clearance was slower, background greater and in vivo deiodination greater than ^{123}I-MIBG. HED has been shown to localize in pheochromocytomas and neuroblastomas (*53*). High-quality PET images of neuroblastoma are obtained within minutes after injection, and image quality is comparable to ^{123}I-MIBG SPECT images obtained with a multiheaded gamma camera. We have recently reported that EPI is likewise concentrated by pheochromocytomas, and preliminary evidence suggests the same for neuroblastomas (*54*). FIBG has been shown to be concentrated by neuroblastoma cells in culture (*12*). Benzylguanidine labeled with ^{211}At, an alpha particle emitter, has been

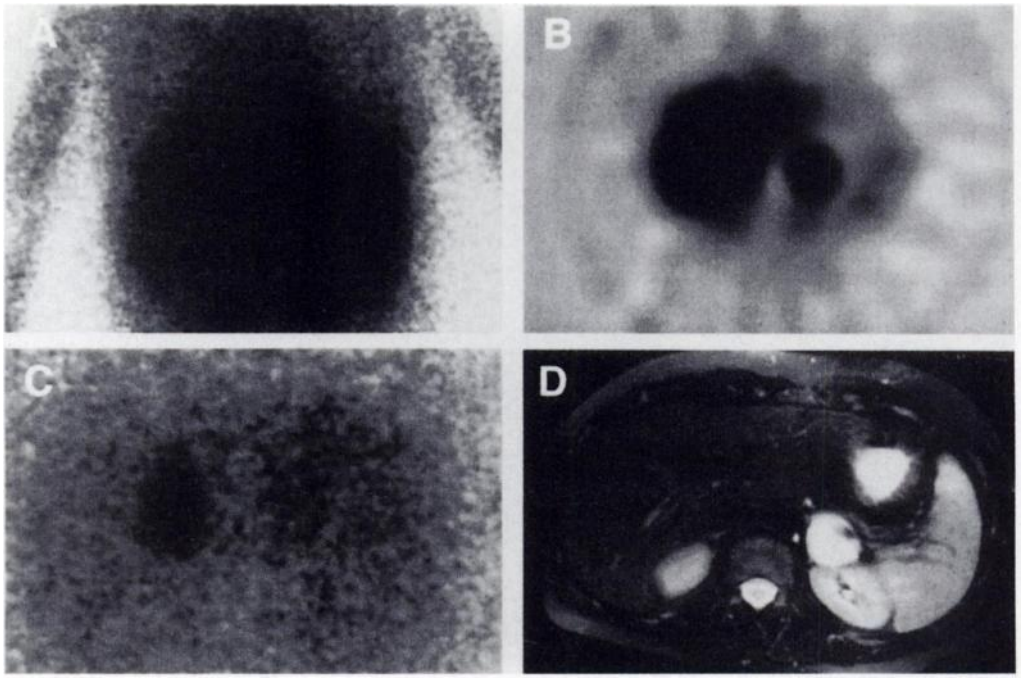

FIGURE 6. A 12-yr-old boy, son of a patient with von Hippel Landau disease and previous resection of a pheochromocytoma, with hypertension and elevated urinary catecholamines and metabolites. Iodine-123-MIBG scan (A-C) and magnetic resonance image (D). (A-C) Posterior planar view of the chest and abdomen at 24 hr tranverse SPECT reconstruction at 24 hr and posterior planar view of the abdomen at 48 hr shows markedly increased uptake in the region of the left adrenal gland consistent with pheochromocytoma. (D) T2-weighted transverse magnetic resonance image demonstrates increased signal intensity from the 3-cm left adrenal mass, consistent with pheochromocytoma.

proposed as a potential radiotherapeutic agent (*15*). These derivatives of MIBG share the type 1 uptake pathway for entry into the cell. However, the extent and mechanism of retention may vary according to the physicochemical properties of the individual agents.

Comparison with Other Imaging Agents for Neuroblastoma

Gallium-67 is not commonly used for imaging of neuroblastoma. However, nearly 80% sensitivity for detection of the primary tumor has been reported, although gallium imaging did not visualize skeletal involvement (*55*). Thallium-201 has been useful for imaging a variety of soft tissue tumors but localizes poorly in neuroblastoma (*56*).

Many neuroendocrine tumors express somatostatin receptors, of which there are now recognized to be at least five subtypes. The currently available ^{111}In-DTPA-pentetreotide (Octreoscan) binds primarily to the subtype 2 receptor. This radiotracer depicts the majority of neuroblastomas and pheochromoytomas but appears inferior to MIBG for imaging of both tumors (*57–59*). Octreoscan uptake by neuroblastoma may be associated with a somewhat better prognosis than for tumors nonavid for somatostatin analogs. Visualization of neuroblastomas in the abdomen and pelvis can be impaired by the marked normal hepatic, splenic, renal and bowel uptake of this agent. In contrast to MIBG, the uptake of which is highly specific for neuroblastoma and pheochromocytoma, Octreoscan images many types of neuroendocrine tumors, including carcinoids, islet cell tumors, pituitary adenomas and medullary carcinoma of the thyroid. Furthermore, a wide range of non-neuroendocrine tumors may also be visualized, including lymphomas and small cell carcinoma of the lung. Inflammatory infiltrates may also show uptake.

Fluorine-18-fluorodeoxyglucose (FDG) is useful in the evaluation of several malignancies, including those of the brain, breast, lung and colon. FDG also is concentrated by most neuroblastomas and pheochromocytomas (*60*). Enhanced glycolytic metabolism is a characteristic of most common neoplasms. Unlike MIBG accumulation into the neuroblastoma cell, FDG uptake does not depend on Type 1 catecholamine uptake. We recently compared the use of FDG with MIBG in patients with neuroblastoma. Most neuroblastomas concentrate FDG and uptake before therapy is often intense. Most neuroblastomas undergoing therapy still accumulated FDG but less so than before therapy. Both before and after therapy, MIBG images better depicted the primary tumor and metastases. FDG imaging in neuroblastomas is most valuable for the depiction of those tumors which fail to concentrate MIBG.

The ^{131}I-labeled monoclonal antibody 3F8 is directed against the ganglioside GD2, which is present in high concentration in most neuroblastomas yet absent from most normal tissues (*61*). This agent has been used to select patients eligible for therapy with high doses of the radiolabeled compound. Biodistribution studies show localization in primary tumors and metastases, and this agent may be more sensitive than ^{131}I-MIBG for depiction of disease. Both the radiolabeled and nonradiolabeled form may be active against neuroblastoma. Several other monoclonal antibodies are under investigation (*62–64*). A ^{99m}Tc-labeled antibody may also be useful, especially for depicting non-MIBG avid bone metastases (*62*).

CONCLUSION

Neuroblastoma remains a major challenge to pediatric oncology. MIBG and related tracers have high sensitivity and specificity for this tumor (and for the rare childhood pheochromocytoma, which is clinically seldom confused with neuroblastoma). Iodine-131-MIBG is approved for clinical use in the U.S., and ^{123}I-MIBG is synthesized for local use in many institutions and is widely available in Europe. Most tracers that have been evaluated in neuroblastoma have been compared to MIBG, which remains the scintigraphic standard, and while attempts to develop other tracers continue, MIBG remains the single best radiotracer for imaging neuroblastoma. Though ^{131}I-MIBG may not be optimal due to the imaging characteristics of the ^{131}I label, it has a well established role in the staging and monitoring of neuroblastoma.

ACKNOWLEGMENTS

The authors are grateful to Donald M. Wieland, PhD, who developed MIBG and other tracers for evaluation of the sympathetic nervous system that have greatly expanded our knowledge and understanding in this area; James C. Sisson, MD, for intellec-

tual stimulation and guidance and William H. Beierwaltes, MD, without whose insight into and interest in neuroendocrine tumors this work would not have been possible. This work was supported in part by grants R29 CA54216 from the National Cancer Institute and MO1 RR 00042 from the University of Michigan Clinical Research Center.

REFERENCES

1. Wieland DM, Swanson DP, Brown LE, Beierwaltes WH. Imaging the adrenal medulla with an ^{131}I-labeled antiadrenergic agent. *J Nucl Med* 1980;20:155–158.
2. Sisson JC, Frager MS, Valk TW, et al. Scintigraphic localization of pheochromocytoma. *N Engl J Med* 1981;305:12–17.
3. Miller L. Food and Drug Administration grants approval for ^{131}I-MIBG. *J Nucl Med* 1994;35:13N–17N.
4. Berthold F. Overview: biology of neuroblastoma. In: Pochedly C, ed. *Neuroblastoma: tumor biology and therapy*. Boca Raton, FL: CRC Press; 1990:2–27.
5. McEwan AJ, Shapiro B, Sisson JC, Beierwaltes WH, Ackery DM. Radioiodobenzyguanidine for the scintigraphic location and therapy of adrenergic tumors. *Semin Nucl Med* 1985;15:132–153.
6. Korn N, Buswink A, Yu T, Carr EA, Caroll M, Counsell RE. A radioiodinated bretylium analog as a potential agent for scanning the adrenal medulla. *J Nucl Med* 1977;18:87–89.
7. Treuner J, Feine U, Niethammer D, et al. Scintigraphic imaging of neuroblastoma with ^{131}I-iodobenzylguanidine. *Lancet* 1984;8372:333-334.
8. Geatti O, Shapiro B, Sisson JC, et al. Iodine-131 metaiodobenzylguanidine scintigraphy for the location of neuroblastoma: preliminary experience in ten cases. *J Nucl Med* 1985;26:736–42.
9. Shapiro B, Gross MD. Radiochemistry, biochemistry and kinetics of ^{131}I-MIBG and ^{123}I-MIBG: clinical implications of the use of ^{123}I-MIBG. *Med Pediatr Oncol* 1987;15:170–177.
10. Sisson JC, Shapiro B, Hutchinson RJ, Shulkin BL, Zempel S. Survival of patients with neuroblastoma treated with ^{125}I-MIBG. *Am J Clin Oncol* 1996;19:144–148.
11. Ott RJ, Tait D, Flower MA, Babich JW, Lambrecht RM. Treatment planning for ^{131}I-MIBG radiotherapy of neural crest tumours using ^{124}I-MIBG positron emission tomography. *Br J Radiology* 1992;65:787–91.
12. Vaidynathan G, Sffleck DJ, Zalutsky MR. 4-[^{18}F]fluoro-3-iodobenzylguanidine, a potential MIBG analogue for positron emission tomography. *J Med Chem* 1994;37: 3655–3662.
13. Clerc J, Mardon K, Galons R, et al. Assessing intratumor distribution and uptake with MBBG versus MIBG imaging and targeting xenografted PC12-pheochromocytoma cell line. *J Nucl Med* 1995;36:859–866.
14. Valette H, Loc'h C, Mardon K, et al. Bromine-76-metabromobenzylguanidine: a PET radiotracer for mapping sympathetic nerves of the heart. *J Nucl Med* 1993;34:1739–1744.
15. Vaidyanathan G, Strickland DK, Zalutsky MR. Meta-[^{211}At]astatobenzylguanidine: further evaluation of a potential therapeutic agent. *Int J Cancer* 1994;57:908–913.
16. Gelfand MJ. Iodine-123-MIBG and ^{131}I-MIBG imaging in children with neuroblastoma [Abstract]. *J Nucl Med* 1996;37(suppl):35P.
17. Geatti O, Shapiro B, Shulkin B, Hutchinson R, Sisson JC. Gastrointestinal iodine-131-meta-iodobenzylguanidine activity. *Am J Physiol Imaging* 1988;3:188–191.
18. Jacques S, Tobes MC, Sisson JC, et al. Comparison of the sodium dependence of uptake of meta-iodobenzylguanidine and norepinephrine into cultured bovine adrenomedullary cells. *Mol Pharmacol* 1984;26:539–546.
19. Smets LA, Loesberg C, Janssen M, Metwally EA, Huiskamp R. Active uptake and extravesicular storage of m-iodobenzylguanidine in human neuroblastoma SK-N-SH cells. *Cancer Res* 1989;49:2941–2944.
20. Smets LA, Janssen M, Metwally E, Loesberg C. Extragranular storage of the neuron blocking agent meta-iodobenzylguanidine (MIBG) in human neuroblastoma cells. *Biochem Pharmacol* 1990;39:1959–1964.
21. Montaldo PG, Raffaghello L, Guarnaccia F, Pistoia V, Garaventa A, Ponzoni M. Increase of metaiodobenzylguanidine uptake and intracellular half-life during differentiation of human neuroblastoma cells. *Int J Cancer* 1996;67:95–100.
22. Khafagi FA, Shapiro B, Fig LM, Mallette S, Sisson JC. Labetalol reduces iodine-131 MIBG uptake by pheochromocytoma and normal tissues. *J Nucl Med* 1989;30:481–489.
23. Paltiel HJ, Gelfand MJ, Elgazzar AH, et al. Neural crest tumors: iodine-123-MIBG imaging in children. *Radiology* 1994;190:117–121.
24. Ruffini V, Fisher GA, Shulkin BL, Sisson JC, Shapiro B. Iodine-123-MIBG imaging of neuroblastoma: utility of SPECT and delayed imaging. *J Nucl Med* 1996;37:1464–1468.
25. Nakajo M, Shapiro B, Copp J, et al. The normal and abnormal distribution of the adrenomedullary imaging agent m[^{131}I]iodobenzylguanidine (^{131}I-MIBG) in man: evaluation by scintigraphy. *J Nucl Med* 1983;24:672–682.
26. Bonnin F, Lumbroso J, Tenenbaum F, Hartmann O, Parmentier C. Refining interpretation of MIBG scans in children. *J Nucl Med* 1994;35:803–810.
27. Hattner RS, Pounds TR, Matthay KK. Normal cerebellar MIBG localization. Implications in the interpretation of delayed scans. *Clin Nucl Med* 1994;19:985–988.
28. Shulkin BL, Shen SW, Sisson JC, Shapiro B. Iodine-131-MIBG scintigraphy of the extremities in metastatic pheochromocytoma and neuroblastoma. *J Nucl Med* 1987; 28:315–318.
29. Shapiro B, Shulkin BL, Hutchinson RJ, Bass JC, Gross MD, Sisson JC. Locating neuroblastoma in the opsoclonus-myoclonus syndrome. *J Nucl Med Biol* 1994;38:545–555.
30. Parisi MT, Hattner RS, Matthay KK, Berg BO, Sandler ED. Optimized diagnostic strategy for neuroblastoma in opsoclonus-myoclonus. *J Nucl Med* 1993;34:1922–1926.
31. Suc A, Lumbroso J, Rubie H, et al. Metastatic neuroblastoma in children older than one year: prognostic significance of the initial metaiodobenzylguanidine scan and proposal for a scoring system. *Cancer* 1996;77:805–811.
32. Turba E, Fagioli G, Mancini AF, Rosito P, Galli A, Alvisi P. Evaluation of stage 4 neuroblastoma patients by means of MIBG and ^{99m}Tc-MDP scintigraphy. *J Nucl Biol Med* 1993;37:107–114.
33. Englaro EE, Gelfand MJ, Harris RE, Smith HS. Iodine-131-MIBG imaging after bone marrow transplantation for neuroblastoma. *Radiology* 1992;182:515–520.
34. Lumbroso JD, Guermazi F, Hartmann O, et al. Meta-iodobenzylguanidine (MIBG) scans in neuroblastoma: sensitivity and specificity, a review of 115 scans. *Prog Clin Biol Res* 1988;271:689–705.
35. Feine U, Muller-Schauenburg W, Treuner J, Klingebiel T. Metaiodobenzylguanidine (MIBG) labeled with ^{123}I/^{131}I in neuroblastoma diagnosis and follow-up treatment with a review of the diagnostic results of the International Workshop of Pediatric Oncology held in Rome, September 1986. *Med Pediatr Oncol* 1987; 15:181–187.
36. Heyman S, Evans AE, D'Angio GJ. Iodine-131-metaiodobenzylguanidine: diagnostic use in neuroblastoma patients in relapse. *Med Pediatr Oncol* 1988;16:337–340.
37. Schmiegelow K, Simes MA, Agertoft L, et al. Radio-iodobenzylguanidine scintigraphy of neuroblastoma: conflicting results, when compared with standard investigations. *Med Pediatr Oncol* 1989;17:127–130.
38. Troncone L, Rufini V, Danza FM, et al. Radioiodinated metaiodobenzylguanidine (^{131}I-MIBG) scintigraphy in neuroblastoma: a review of 160 studies. *J Nucl Med Allied Sci* 1990;34:279–288.
39. Shulkin BL, Shapiro B. Radioiodinated MIBG in the management of neuroblastoma. In: Pochedly C, ed. *Neuroblastoma tumor biology and therapy*. Boca Raton, FL: CRC Press; 1990:171–198.
40. Andrich MP, Shalaby-Rana E, Movassaghi N, Majd M. The role of iodine-131-metaiodobenzylguanidine scanning in the correlative imaging of patients with neuroblastoma. *Pediatrics* 1996;97:246–250.
41. Simon A, Hoefnagel CA, deKraker J, et al. Iodine-123-MIBG or ^{131}I-MIBG for imaging of neuroblastoma [Abstract]. *Eur J Nucl Med* 1992;19:589.
42. Gelfand MJ, Elgazzar AH, Kriss VM, Masters P, Golsch GJ. Iodine-123-MIBG SPECT versus planar imaging in children with neural crest tumors. *J Nucl Med* 1994;35:1753–1757.
43. Shulkin BL, Shapiro B, Hutchinson RJ. Iodine-131-metaiodobenzylguanidine and bone scintigraphy for the detection of neuroblastoma. *J Nucl Med* 1992;33:1735–1740.
44. Gordon I, Peters AM, Gutman A, Morony S, Dicks-Mireaux C, Pritchard J. Skeletal assessment in neuroblastoma—the pitfalls of iodine-123-MIBG scans. *J Nucl Med* 1990;31:129–134.
45. Hadj-Djilani NL, Lebtahi NE, Delaloye AB, Laurini R, Beck D. Diagnosis and follow-up of neuroblastoma by means of iodine-123-metaiodobenzylguanidine scintigraphy and bone scan, and the influence of histology. *Eur J Nucl Med* 1995;22:322–329.
46. Osmanagaoglu K, Lippens M, Benoit Y, Obrie E, Schelstraete K, Simons M. A comparison of iodine-123 meta-iodobenzylguanidine scintigraphy and single bone marrow aspiration biopsy in the diagnosis and follow-up of 26 children with neuroblastoma. *Eur J Nucl Med* 1993;20:1154–1160.
47. Corbett R, Olliff J, Fairley N, et al. A prospective comparison between magnetic resonance imaging, meta-iodobenzylguanidine scintigraphy and marrow histology/cytology in neuroblastoma. *Eur J Cancer* 1991;27:1560–1564.
48. Giammarile F, Lumbroso J, Ricard M, et al. Radioiodinated metaiodobenzylguanidine in neuroblastoma: influence of high dose on tumour site detection. *Eur J Nucl Med* 1995;22:1180–1183.
49. Leung A, Shapiro B, Hattner R, et al. The specificity of radioiodinated MIBG for neural crest tumors in childhood. *J Nucl Med* 1997;38:1352–1357.
50. Khafagi F, Shapiro B, Fischer M, et al. Pheochromocytomas and functioning paraganglioma in childhood and adolescence: role of iodine-131-metaiodobenzylguandine. *Eur J Nucl Med* 1991;18:191–198.
51. Lynn MD, Shapiro B, Sisson JC, et al. Portrayal of pheochromocytoma and normal human adrenal medulla by m-[^{123}I]iodomethylguanidine: concise communication. *J Nucl Med* 1984;25:436–440.
52. Shulkin B, Shapiro B, Tobes M, et al. Iodine-123–4-Amino-3-iodobenzylguanidine (^{123}I-AIBG), a new sympatho-adrenal imaging agent: comparison with ^{123}I-meta-iodobenzylguanidine. *J Nucl Med* 1986;27:1138–1142.
53. Shulkin BL, Wieland DM, Baro ME, et al. PET hydroxyephedrine imaging of neuroblastoma. *J Nucl Med* 1996;37:16–21.
54. Shulkin BL, Wieland DM, Shapiro B, Sisson JC. PET epinephrine studies of pheochromocytoma [Abstract]. *J Nucl Med* 1995:36(suppl):22P–23P.
55. Garty I, Friedman A, Sandler MP, Kedar A. Neuroblastoma: imaging evaluation by sequential ^{99m}Tc-MDP, ^{131}I-MIBG and ^{67}Ga-citrate studies. *Clin Nucl Med* 1989;14: 515–522.
56. Howman-Giles R, Uren RF, Shaw PJ. Thallium-201 scintigraphy in pediatric soft-tissue tumors. *J Nucl Med* 1995;36:1372–1376.
57. Sautter-Bihl ML, Dorr U, Schilling F, Treuner J, Bihl H. Somatostatin receptor imaging: a new horizon in the diagnostic management of neuroblastoma. *Semin Oncol* 1994;21(suppl 13):38–41.
58. Manil L, Edeline V, Lumbroso J, Lequen H, Zucker JM. Indium-111-pentetreotide scintigraphy in children with neuroblast-derived tumors. *J Nucl Med* 1996;37:893–896.
59. Lauriero F, Rubini G, D'Addabbo F, Rubini D, Schettini F, D'Addabbo A. Iodine-131-MIBG scintigraphy of neuroectodermal tumors. Comparison between ^{131}I MIBG and ^{111}In DTPA-octreotide. *Clin Nucl Med* 1995;20:243–249.
60. Shulkin BL, Hutchinson RJ, Castle VP, Yanik GA, Shapiro B, Sisson JC. Neuroblastoma: positron emission tomography with 2[^{18}F]-fluoro-2-deoxy-D-glucose compared with metaiodobenzylguanidine scintigraphy. *Radiology* 1996;199:743–750.
61. Yeh SD, Larson SM, Burch L, et al. Radioimmunodetection of neuroblastoma with iodine-131-3F8: correlation with biopsy, iodine-131-metaiodobenzylguanidine and standard diagnostic modalities. *J Nucl Med* 1991;32:769–776.
62. Berthold F, Waters W, Sieverts H, Linden A. Immunoscintigraphic imaging of

MIBG-negative metastases in neuroblastoma. *Am J Pediatr Hematol Oncol* 1990;12: 61–62.
63. Horne T, Granowska M, Dicks-Mireaux C, et al. Neuroblastoma imaged with ^{123}I meta-iodo-benzylguanidine and with ^{123}I-labeled monoclonal antibody, UJ13A, against neural tissue. *Br J Radiol* 1985;58:476–480.
64. Handgretinger R, Anderson K, Lang P, et al. A phase I study of human/mouse chimeric antiganglioside GD2 antibody ch14.18 in patients with neuroblastoma. *Eur J Cancer* 1995;31A:261–267.
65. Swanson DP, Carey JE, Brown LE, et al. Human absorbed dose calculations for iodine-131 and iodine-123-labeled meta-iodobenzylguanidine (MIBG): a potent myocardial and adrenal medulla imaging agent. In: *Proceedings of the Third International Symposium of Radiopharmaceutical Dosimetry*. Oak Ridge, TN: Oak Ridge Associated Universities; 1981:213–224.
66. Shapiro B. MIBG in the Diagnosis and Therapy of Neuroblastoma and Pheochromocytoma. Proceedings of the International Symposium on Recent Advances in Nuclear Medicine; 1987:11–20.
67. Hoefnagel CA, Voute PA, DeKraker J, et al. Radionuclide diagnosis and therapy of neural crest tumors using iodine-131-metaiodobenzyl-guanidine. *J Nucl Med* 1987;28: 308–314.
68. Lumbroso J, Hartmann O, Leerle J, et al. Scintigraphic detection of neuroblastoma using ^{131}I and ^{123}I labelled metaiodobenzyl-guanidine [Abstract]. *Eur J Nucl Med* 1985;11:A16.
69. Heyman S, Evans AE. Iodine-131-metaiodobenzylguanidine (I-131-MIBG) in the diagnosis of neuroblastoma [Abstract]. *J Nucl Med* 1986;27:931.
70. Munkner T. Scintigraphy of neuroblastoma. *Nuklearmedizin* 1986(suppl):436–438.
71. Feine U, Treuner J, Niethammer D, et al. Erste untenshungen zur scintigraphischen darstellung von neuroblastomen mit 131-J-meta-benzylguanidin. *Nuc Compact* 1984; 15:23–26.
72. Fischer M, Galanski M, Winterberg B, Vette H. Localization procedures in pheochromocytoma and neuroblastoma. *Cardiology* 1985;72(suppl 1):143–146.
73. Edeling CJ, Buchler Frederiksen P, Kamper J, Jeppesen R. Diagnosis and treatment of neuroblastoma using metaiodobenzylguanidine. *Clin Nucl Med* 1987;8:632–637.
74. Muller-Gartner HW, Erttmann R, Helmke K. Die Szintigraphie mit Radiojod-[Meta-Jod-Benzylguanidin] in der Diagnostik des Neuroblastoms. *Nuklearmedizin* 1985;24: 222–226.
75. Kimmig B, Brandeis WE, Eisenhut M, Ludwig R, Adolph J. Szintigraphische Diagnostik des Neuroblastoms mit meta-Jod-Benzylguanidin. *Klin Padiat* 1986;198: 224–229.
76. Odano I, Masayuki T, Saka K. Significance of I-131 meta-iodobenzylguanidine scintigraphy in diagnosing neuroblastoma. *Kaku Igaku* 1986;11:1685–1688.
77. Caballero O, Ferris J, Verdeguer A, Esquembre C, Castel V. Iodine-131 metaiodobenzylguanidine. *J Nucl Med* 1986;27:868–869.
78. Hadley GP, Rabe E. Scanning with iodine-131-MIBG in children with solid tumors: an initial appraisal. *J Nucl Med* 1986;27:620–626.
79. Feine U, Muller-Schauenburg W, Treuner J, Klingebiel T. Metaiodobenzylguanidine (MIBG) Labeled with ^{123}I/^{131}I in neuroblastoma diagnosis and follow-up treatment with a review of the diagnostic results of the International Workshop of Pediatric Oncology Held in Rome, September 1986. *Med Pediatr Oncol* 1987;15:181–187.